Guidelines and **R**ecommendations for **I**ntegrating **S**pecific **P**rofiled steel sheets in the **E**urocodes (**GRISPE**)

WP2 Doc 1 Version 02

Background Document

Working Package 2

Deliverable D 2.1

Guidelines and Recommandations for Integrating Specific Profiled Steels sheets in the Eurocodes (GRISPE)

Project co-funded under the Research Fund for Coal and Steel
Grant agreement No RFCS-CT-2013-00018
Proposal No RFS-PR-12027

Author(s)	
C. Fauth, KIT	

Drafting history	
Draft Version 1	*28th November 2013*
Final Version 1	*30th November 2013*

Dissemination Level		
PU	*Public*	
PP	*Restricted to the Commission Services, the Coal and Steel Technical Groups and the European Committee for Standardisation (CEN)*	
RE	*Restricted to a group specified by the Beneficiaries*	
CO	*Confidential, only for Beneficiaries (including the Commission services)*	***X***

Verification and Approval
Coordinator: David Izabel, SNPPA, 30.11.2013
WP2 Leader: Rainer Holz, IFL. 30.11.2013
Other Beneficiaries

Deliverable	
D 2.1 Backround Document	***Due date: 30th Nov. 2013*** ***Completion date: 30th Nov. 2013***

Summary

1 Liner Trays

1.1 Component description

A liner tray is a trough-like cold formed steel component with a wide flange with two webs and two smaller flanges. The two small flanges are stiffened with outward profiles which span at right angle to the span of the liner trays, for example trapezoidal or corrugated sheets. There could be also wall panels instead of the trapezoidal or corrugated profiles. The width is normally between 500 mm and 600 mm. The height is normally between 90 mm and 160 mm. Typically they are used for inner sheets of walls, but they can also be used for roof lower sheets. To increase the load bearing capacity the flanges and webs are reinforced with stiffeners. The liner trays can be spanning vertically or horizontally. When they are spanning horizontally they form a two layer built-up cladding system. When they span vertically they build a cassette wall system.

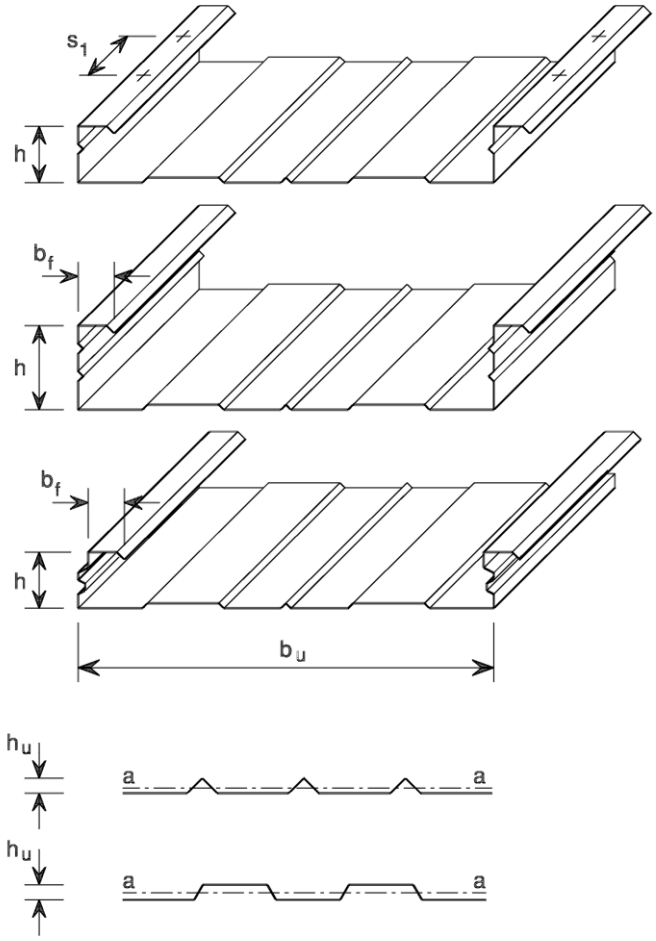

Fig.1: Typical design of liner trays [DIN EN 1993-1-3]

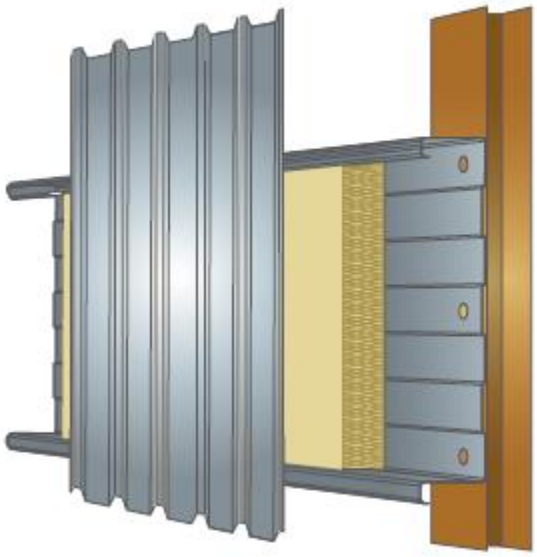

Fig. 2a: Typically two layer build-up wall cladding system [product catalog of Joris IDE]

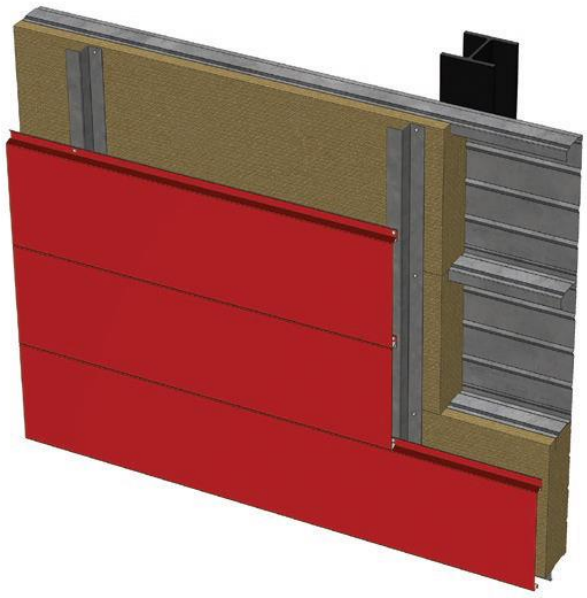

Fig. 2b: Two layer build-up wall cladding system with outward panels instead of trapezoidal sheets [product catalog of Bacacier]

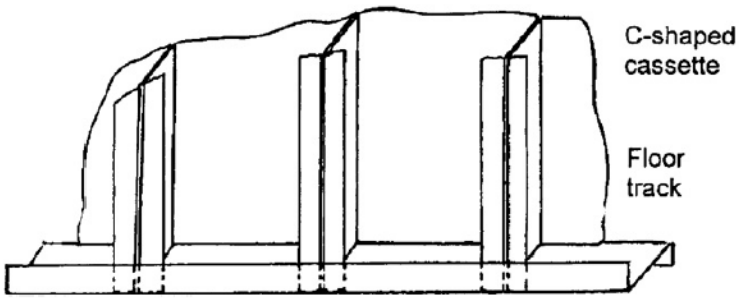

Fig. 2c: Cassette wall construction [1]

The determination of the load bearing capacity is carried out via experiments. In Germany the test procedures are governed by the following documents:

- DIN EN 1993-1-3
- DIN EN 1993-1-3/NA
- DIN 18807-2
- DIN 18807-2/A1
- "Ergänzende Prüfgrundsätze für Stahlkassettenprofiltafen"

1.2 Design model according to DIN EN 1993-1-3

A design method is given in Eurocode EN 1993-1-3. Axial compression is not explicitly considered in En 1993-1-3. The design procedure is similar to that for bending with the narrow flanges in compression.
For wide flange and web, the effective width approach will be applied, while for the smaller flanges and the adjacent edge stiffener the iterative procedure has to be used.
The resistance of the webs is given in section 6.1.5 "shear force" and for local transverse forces section 6.5.11 "Combined bending moment and local load or support reaction". The load bearing capacity in bending is given in section 10.2.2 "Moment resistance". The shear resistance should be determined by the following expression

$$V_{b,Rd} = \frac{\frac{h_w}{\sin\varphi} * t * f_{bv}}{\gamma_{mo}}$$

The shear buckling strength f_{bv} can be determined with the following table

Relative web slenderness	Web without stiffening at the support	Web with stiffening at the support [1)]
$\bar{\lambda}_w \leq 0{,}83$	$0{,}58\ f_{yb}$	$0{,}58\ f_{yb}$
$0{,}83 < \bar{\lambda}_w < 1{,}40$	$0{,}48 f_{yb} / \bar{\lambda}_w$	$0{,}48 f_{yb} / \bar{\lambda}_w$
$\bar{\lambda}_w \geq 1{,}40$	$0{,}67 f_{yb} / \bar{\lambda}_w^2$	$0{,}48 f_{yb} / \bar{\lambda}_w$
[1)] Stiffening at the support, such as cleats, arranged to prevent distortion of the web and designed to resist the support reaction.		

Table 1: shear buckling strength f_{bv} according to EN 1993-1-3

The relative web slenderness $\bar{\lambda}_w$ for webs without longitudinal stiffeners can be determined with

$$\bar{\lambda}_w = 0{,}346 * \frac{s_w}{t} * \sqrt{\frac{f_{yb}}{E}}$$

for webs with longitudinal stiffeners the web slenderness is given below

$$\bar{\lambda}_w = 0{,}346 * \frac{s_d}{t} * \sqrt{\frac{5{,}34 * f_{yb}}{\kappa_\tau * E}}$$

with

$$\kappa_\tau = 5{,}34 + \frac{2{,}10}{t} * \left(\frac{\sum I_s}{s_d}\right)^{1/3}$$

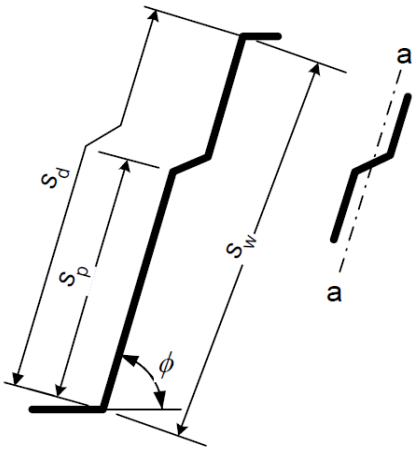

Fig. 3: Longitudinally stiffened web

The resistance in bending $M_{c,Rd}$ is given below when the following conditions are complied:

- the geometry values are within the following range (see Ill. 4)
- the depth of the corrugations of the wide flange does not exceed h/8, where h is the overall depth of the liner tray

0,75 mm	≤	t_{nom}	≤	1,5 mm
30 mm	≤	b_f	≤	60 mm
60 mm	≤	h	≤	200 mm
300 mm	≤	b_u	≤	600 mm
		I_a / b_u	≤	10 mm^4 / mm
		s_1	≤	1000 mm

Fig. 4: Range of validity

If the conditions are not fulfilled the determination of the resistance can be carried out by testing. When the wide flange is in compression you should determine the moment resistance with the step by step method given in the following figure

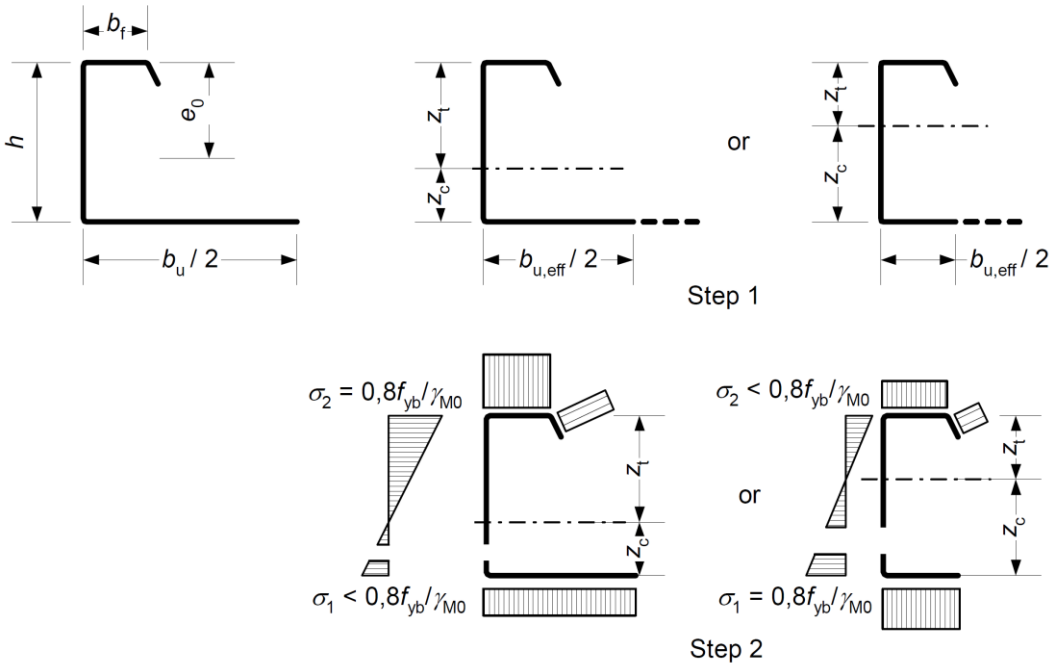

Fig. 5: Determination of moment resistance – wide flange under compression

- Step 1: Determination of the centroid of the cross-section considering the effective areas in cross-sections under compression (Eurocode EN 1993-1-5) with the effective areas of the wide flange and the complete area of the web
- Step 2: Determine the centroid of the new effective cross-section with the effective areas of the web, then determine the moment resistance $M_{c,Rd}$:

$$M_{c,Rd} = 0{,}8 * \frac{W_{eff,min} * f_{yb}}{\gamma_{mo}}$$

When the wide flange is in tension you should determine the moment resistance with the step by step method given in the following figure

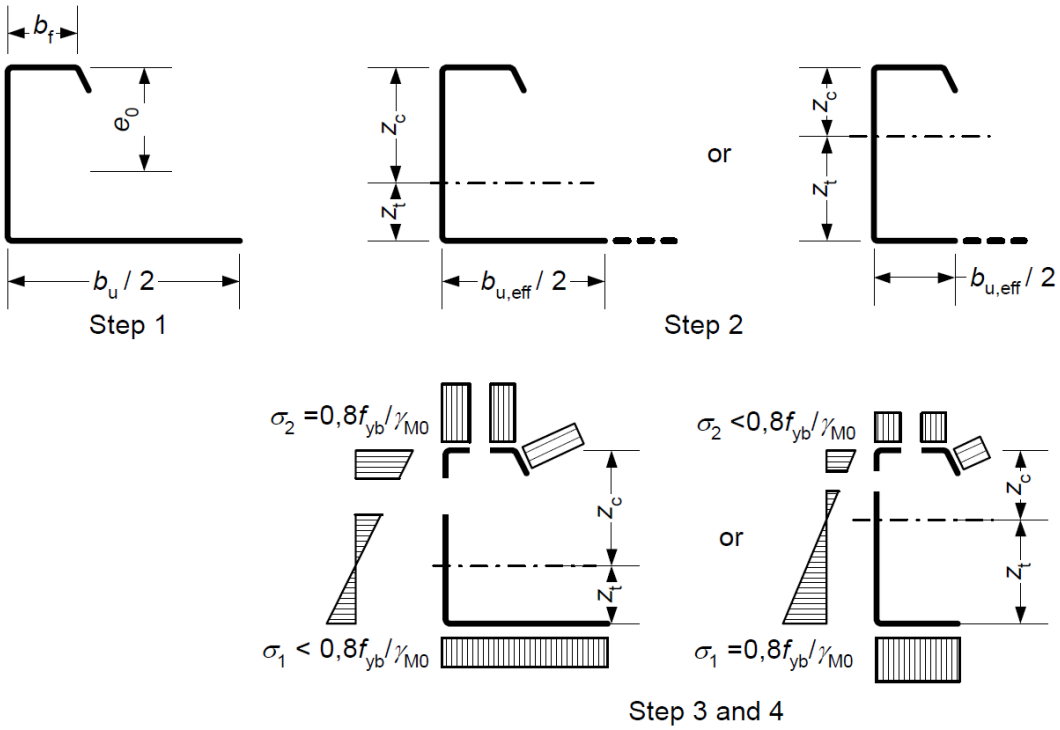

Fig. 6: Determination of moment resistance – wide flange under tension

- Step 1: Determine the centroid of the whole cross-section (fully effective wide flange and web)
- Step 2: Determine the effective width of the wide flange $b_{u,eff}$ (considering flange curling)

$$b_{u,eff} = \frac{53{,}3 * 10^{10} * e_0{}^2 * t^3 * t_{eq}}{h * L * b_u{}^3}$$

with

$t_{eq} = (12 * I_a / b_u)^{1/3}$

- Step 3: Determination of the centroid of the cross-section considering the effective areas in cross-sections under compression (Eurocode EN 1993-1-5) with the effective areas of the wide flange and the complete area of the web
- Step 4: Determine the centroid of the new effective cross-section with the effective areas of the web, then determine the moment resistance $M_{b,Rd}$:

$$M_{b,Rd} = 0{,}8 * \beta_b * \frac{W_{eff,com} * f_{yb}}{\gamma_{mo}} \text{ but } M_{b,Rd} = 0{,}8 * \beta_b * \frac{W_{eff,t} * f_{yb}}{\gamma_{mo}}$$

with the correlation factor β_b:

$\beta_b = 1{,}0$ ($s_1 \leq 300$ mm)
or
$\beta_b = 1{,}15 - s_1/2000$ ($300 \leq s_1 \leq 1000$ mm)

Shear lag need not be considered if $L/b_{u,eff} \geq 25$. Otherwise a reduction of the value with ρ (section 6.1.4.3) needs to be considered.

1.3 Design by testing according to DIN EN 1993-1-3 and DIN 18807

The test procedures in Eurocode EN 1993-1-3 section A2 are presented with profiled sheets, but they are also for liner trays. The test procedures are equal to DIN 18807-2.
There are 4 types of tests, the single span test, the double span test, the internal support test and the end support test. The double span and the internal support test are both for liner trays which are over two or more spans to determine combination of the bending moment and the support reaction resistance. In the following figures the test setups of the single span, the internal support and the end support test are shown.

Single span test:

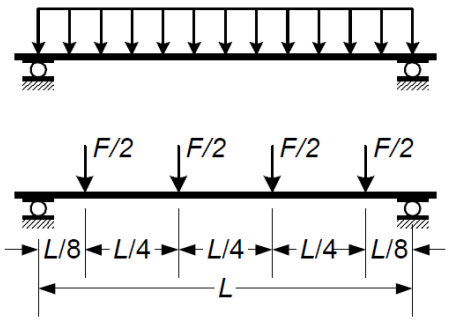

a) Uniformly distributed loading and an example of alternative equivalent line loads

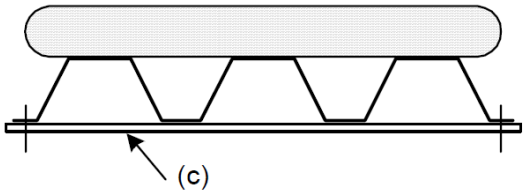

b) Distributed loading applied by an airbag (alternatively by a vacuum test rig)

(c) Transverse tie

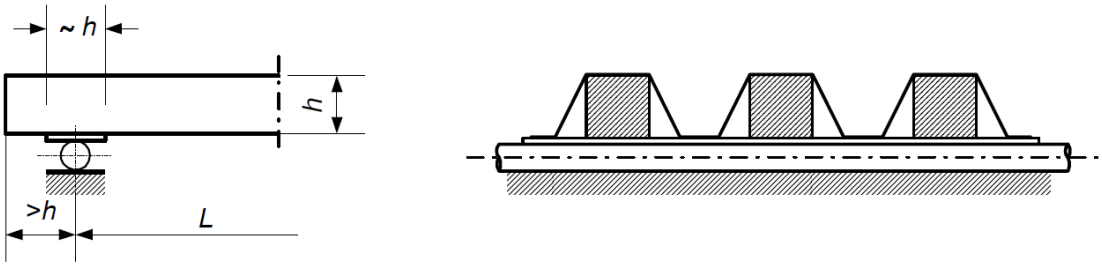

c) Example of support arrangements for preventing distortion

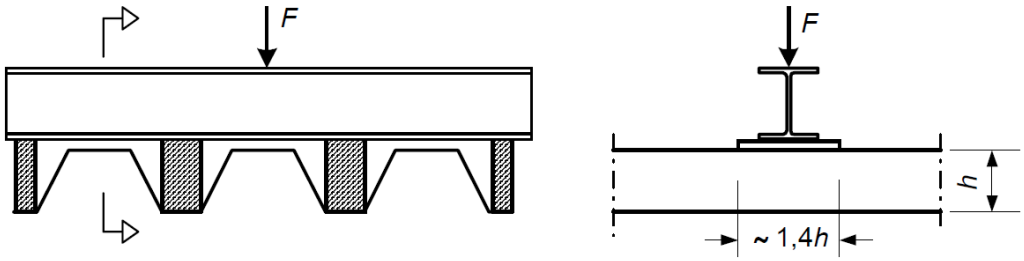

d) Example of method of applying a line load

Fig. 7: Test setup for single span test

Internal support test:

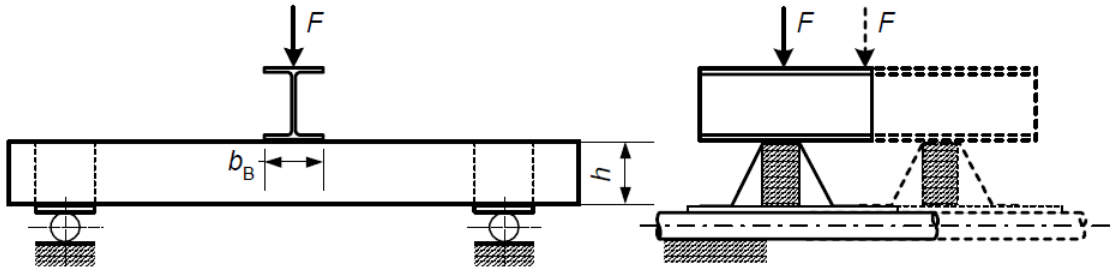

a) Internal support under gravity loading

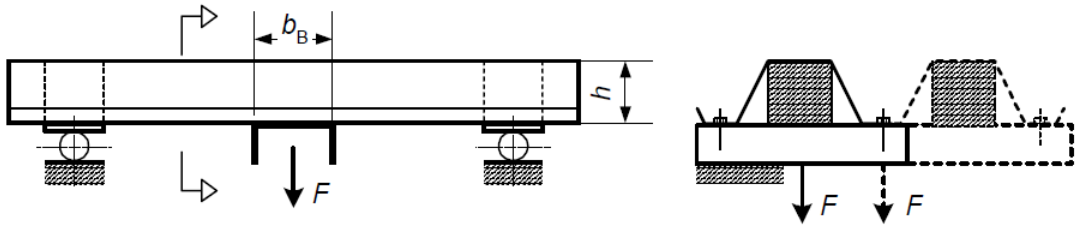

b) Internal support under uplift loading

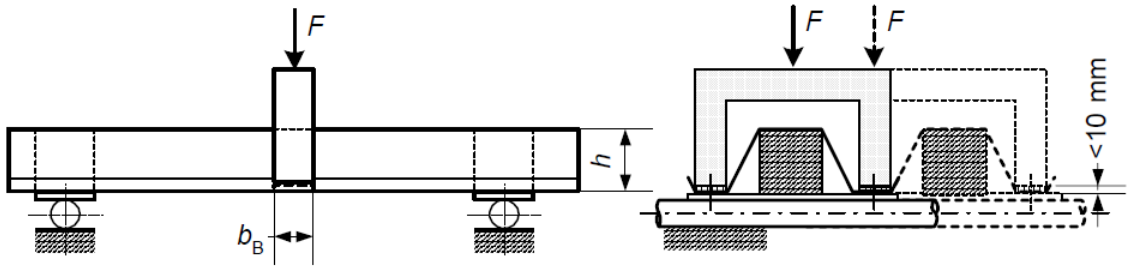

c) Internal support with loading applied to tension flange

Fig. 8: Test setup for the internal support test

End support test:

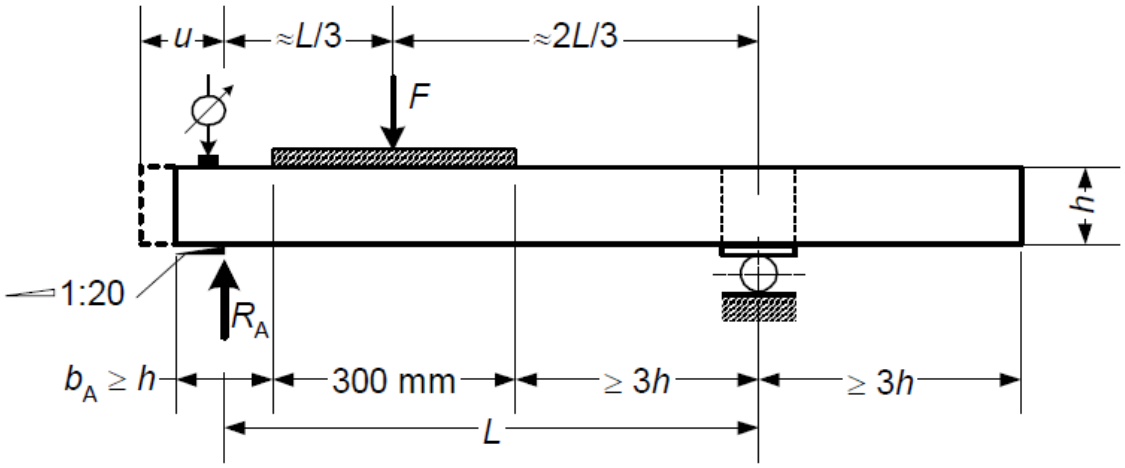

Fig. 9: Test setup for the end support test

In Germany there are additions to the test procedures given by the "Deutsches Institut für Bautechnik" (DIBt) which must be taken into account.

1.4 State of the art

The behavior of liner tray sections under the three primary load systems of axial compression, bending and shear was researched by Baehre in Karlsruhe at the research center of steel, timber and masonry.
The developed test based approach by Baehre [2], [3] and [4] was expanded by studies carried out by Davies at the University of Manchester [5], [6], [7], [8] and [9].
The results are the basis of the design procedure in Eurocode EN 1993-1-3. The geometrical restrictions for these design procedure (see fig. 4) were caused through the limits of the tests by Baehre.
By the design for bending with the wide flange under tension there are three effects which should be considered:

- local buckling of the web and smaller flanges
- distortional buckling of the smaller flanges assembly
- flange curling of the wide flange

The distance s_1 between the fasteners controls the distortional buckling of the small flanges.
In Baehre`s test panels this effect was considered up to a distance s_1 = 1000 mm.
By the design for bending with the wide flange under compression the flange curling of the wide flange interacts with local buckling of the wide flange. The EC 3 deals not with this interaction. The conventional procedure of effective widths should be used.
Because of flange curling there is more scatter between the experimental results and the theory than it is customary by cold formed steel sections in bending. Therefore the EC 3 required a material factor 1,25 instead of 1,0. The higher material factor is considered with a factor 1,00/1,25 = 0,80 in the two formulas for bending resistance $M_{c,Rd}$ and $M_{b,Rd}$.

In [10] Jönsson developed a flange curling model (FCM) and compared it in an analysis of a liner tray with wide flange under tension with a Finite Element Analysis (FEA), the method form EC 3 and tests from Bernard [11].

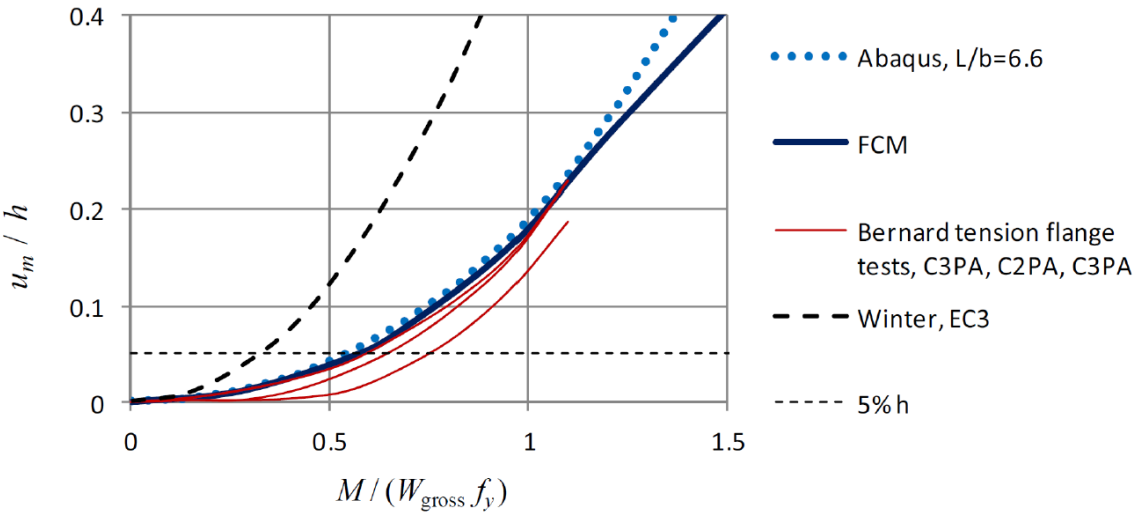

Fig. 10: flange curling displacements of Bernard tests, EC 3, FEA and Jönsson [10]

The conclusion of the author is

- the FCM reproduces the non-linear flange curling displacement behavior for tension flanges for a practical range of slenderness values
- the FCM approximates the stress distribution in the curled flange with reasonable accuracy

- for wide flange in tension the effective moment arm reduction and the effective width have been given
- stiffeners in tension flanges are taken into account by using the full developed width of the flanges
- the use of the FCM in compression flanges should be investigate in further research

The FCM is briefly described in the following lines:
The flange curling phenomenon is initiated by the curvature of the beam, which rotates the axial flange stress resulting towards the neutral axis of the section. The curvature can be found from

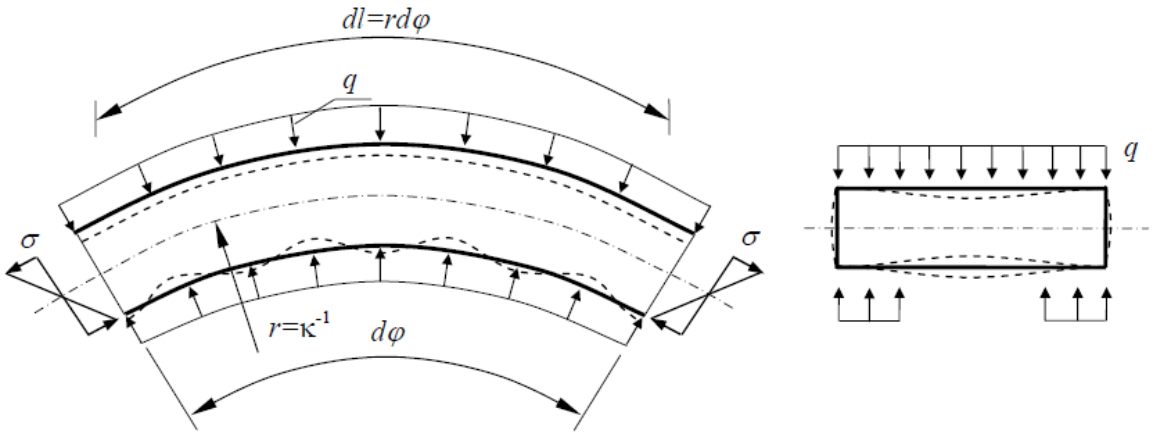

Fig. 11: Second order transverse load action on the flanges

$$\kappa = \frac{\sigma_e}{E * z_e} \quad \text{or} \quad \kappa = \frac{M}{E * I_{ef}}$$

The transverse flange load q is

$$q = t * \sigma * \kappa$$

With the main assumption that “distorted cross-sections remain plain” you can determine the flange stress as a function of the distance x from the corner:

$$\sigma\langle x\rangle = \sigma_e * \left(1 - \frac{u(x)}{z_e}\right)$$

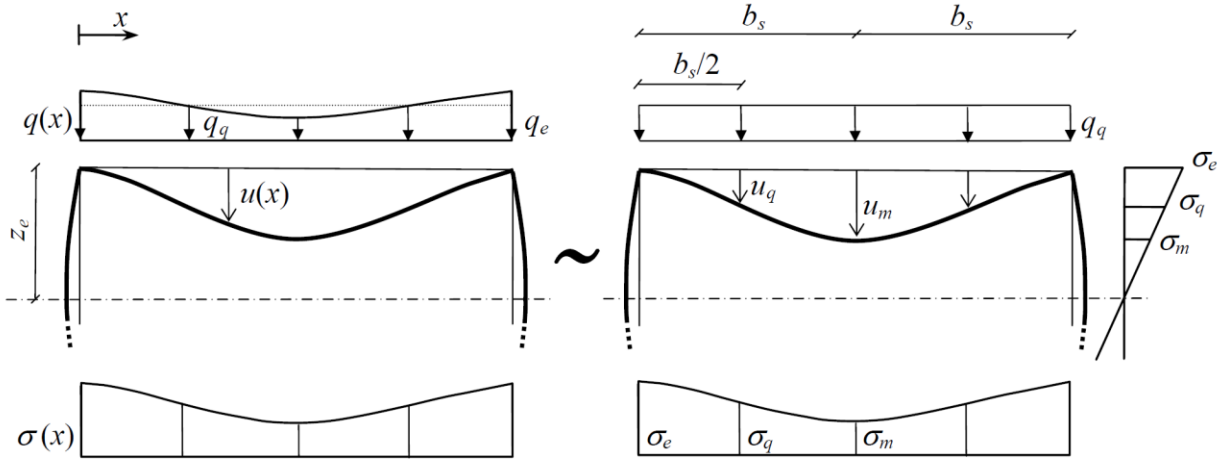

Fig. 12: modelling of second order transverse load action on the flanges [10]

There is a simplification of the problem (see fig. 12b) so that the flange curling load q_q is uniform and determined by the displacement u_q at the quarter points of the flanges

$$q_q = q_e\left(1 - \frac{u_q}{z_e}\right) \quad with \quad q_e = t * \sigma_e * \kappa$$

The displacements from a uniform flange load q_q may be found by using the model shown in the following figure.

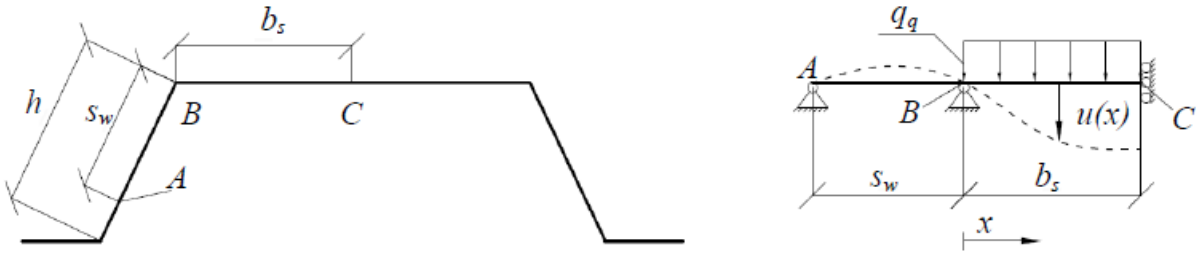

Fig 13: Curling displacements bases on approximate flange support conditions

With the ordinary beam differential equation you can determine the displacement at the quarter point and insert this solution in the previous equation of the flange load q_q so that you can find the approximated uniform flange curling load

$$q_q = q_e * \left(1 - \frac{C_q * q_e}{z_e + C_q * q_e}\right)$$

with

$$q_e = t * \sigma_e * \kappa$$

and

$$C_q = \frac{b_s^4}{24 * D} * \left(\frac{57}{16} - \frac{3}{1 + s_w/(3 * b_s)}\right)$$

with

$$D = \frac{E * t}{12(1 - \nu^2)}$$

With the equation of q_q, C_q and q_e you can find the flange curling displacement with

$$u_q = C_q * q_q$$

The effective widths b_{ef} and the effective moment arm z_{ef} (see fig. 14) can be found by demanding equal moment and equal normal force for the flange curled cross section with the approximate stress distribution.

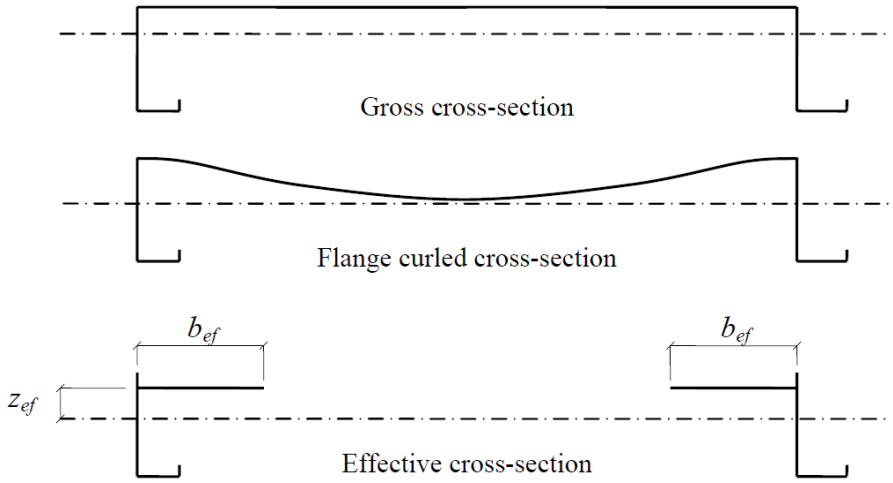

Fig. 14: Flange curling of slender tension flanges

$$\frac{z_{ef}}{z_e} = \frac{{z_e}^2 - 2 * \beta_1 * z_e + \beta_2}{(z_e - \beta_1) * z_e} \quad \text{and} \quad \frac{b_{ef}}{b_s} = \frac{z_e}{z_{ef}}\left(\frac{z_e - \beta_1}{z_e}\right)$$

with

$$\beta_1 = \frac{1 + 2 * s_w/b_s}{15(1 + \frac{s_w}{3 * b_s})} * \left(\frac{q_q * b_s^4}{3 * D}\right)$$

and

$$\beta_2 = \frac{1}{20160} * \left(3968 - \frac{6528}{1 + \frac{s_w}{3 * b_s}} + \frac{2688}{\left(1 + \frac{s_w}{3 * b_s}\right)^2}\right) * \left(\frac{q_q * b_s^4}{3 * D}\right)^2$$

and

$$s_w = 0{,}9 * h$$

These equations can be directly introduced into the iterative scheme for determination of effective cross section properties.

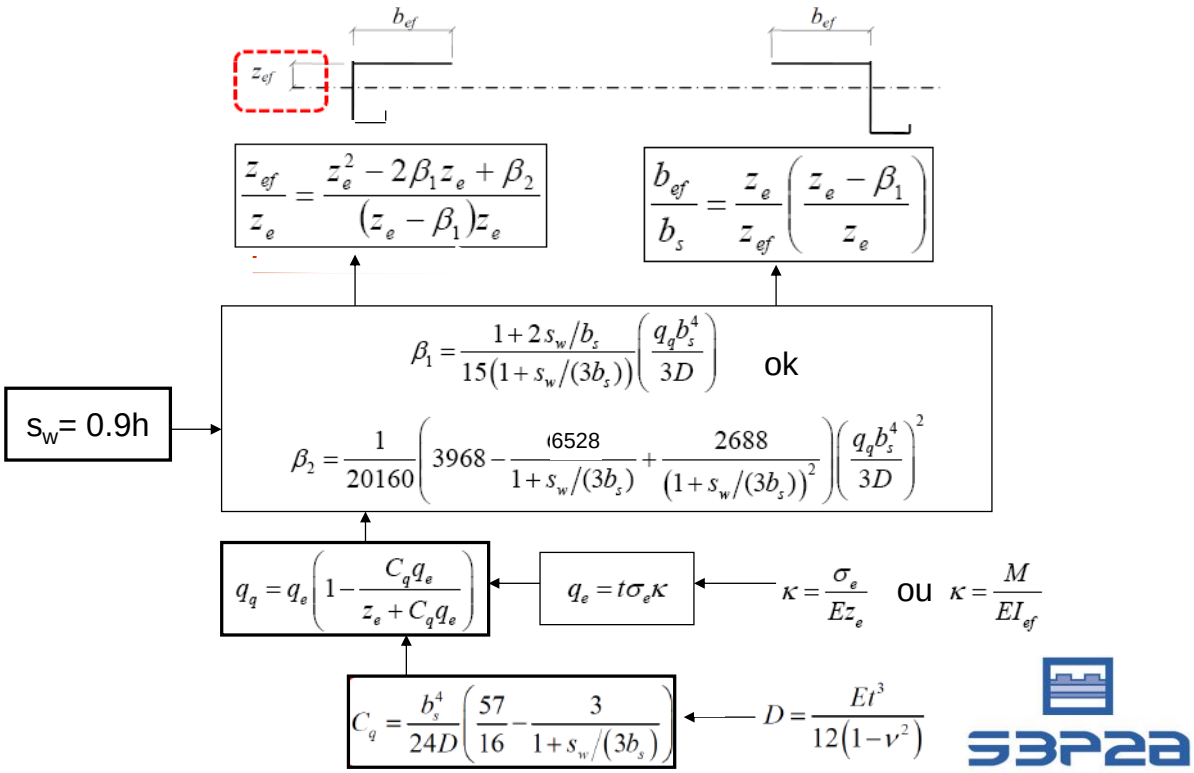

Fig. 15: comparison of FCM

1.5 Conclusion

The restriction of the fasteners distance $s_1 \leq 1000$ mm, which should control distortional buckling, came from the limits of Baehre`s tests (because trapezoidal sheets have normally a width b ≤ 1000 mm). To extend the design rules for spacer distance $s_1 > 1000$ mm a number of series of tests should be performed to analyse the distortional buckling effects. If the spacer distances increase over s_1 = 1000 mm, the "normal" setup liner tray with outward trapezoidal sheets can`t be realized in reality. There must be a cassette wall construction like in figure 2b with outward panels for cladding panels.
The test series will be also used to confirm the FCM method (to acquire data of the flange curling effect to improve the determination of $b_{u,eff}$)
In addition a series of tests should be performed to acquire data of the system behavior (see fig. 16). Dependent of the lateral stiffness of the spacers, this system works like a composite beam with elastic shear bond between the inner layer (liner trays) and the outer layer (profiled sheeting).

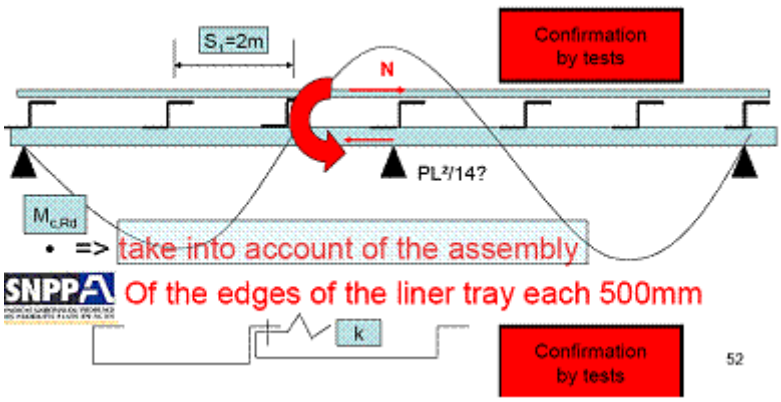

Fig. 16: system behavior of liner trays

2 Assembled profiles

2.1 Component description

There are three types of assemblies (see fig. 10). The resistance of the first joint is equal to a single profile. The resistance by the second and third joint is higher than the load bearing capacity of a single profile. The second joint and third joint are often used to repair buildings or to solve deflection in span. A second reason is to improve the load bearing capacity below snow accumulation
In DIN 18807 there is a design procedure for the fasteners and the web for the clamped joint. In prEN 1090-4 the same procedure is mentioned.

Clamped joint, moment resisting connection (EN 1090-4)	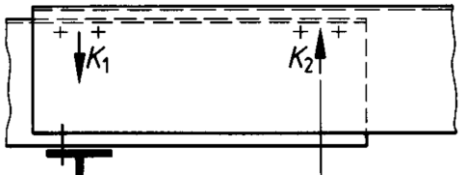
Overlap joint	
Continous profile with local reinforcement	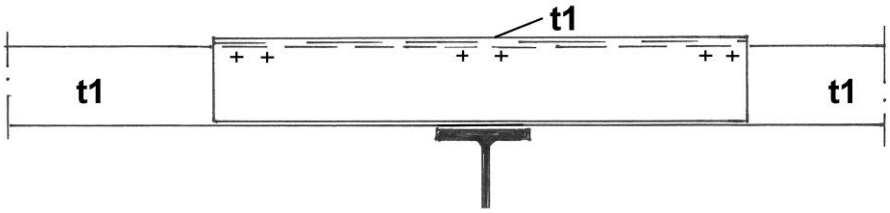

Fig.17: Three various profile assemblies

2.2 DIN 18807 (state of the art)

In DIN 18807 there is a solution for overlapping profiles. They are only allowed at the supports. If powers are to be worn over contact, tests must be performed. In the overlapping field the resistance is equal to a continuous profile. In the following figures 11 and 12 are the two possibilities of this clamped joint.

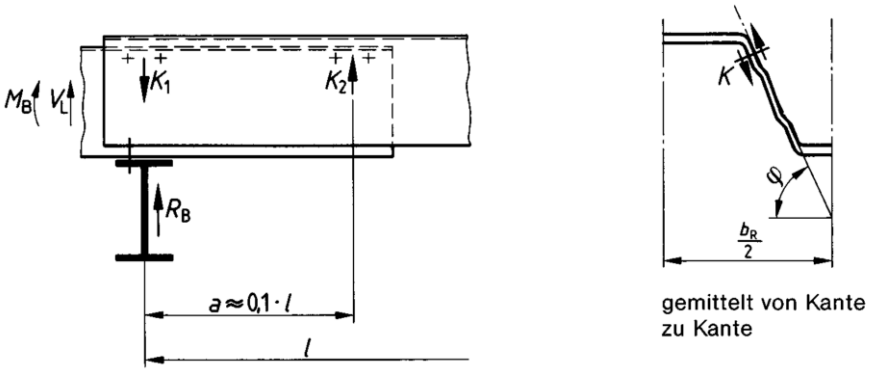

Fig. 18: overlapping profiles according to DIN 18807-3

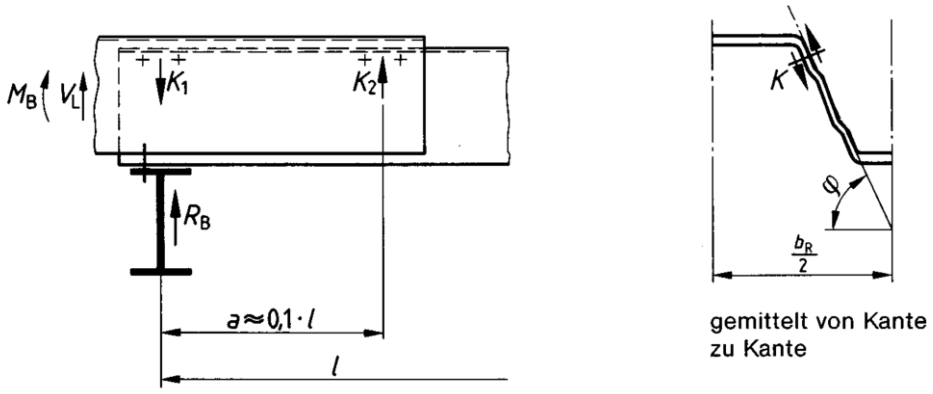

Fig. 19: overlapping profiles according to DIN 18807-3

The force on the fastener is given to

$$K = \max K_i = \frac{|M_B|}{2 * a * \sin\varphi} * b_R \quad \text{(Fig. 11)}$$

or

$$K = \max K_i = \frac{\left|\frac{M_B}{a} + V_L\right|}{2 * \sin\varphi} * b_R \quad \text{(Fig. 12)}$$

A maximum of two fasteners may be recognized in horizontal and vertical direction in each compound (maximum 4 fasteners). The required fastener edge spacings and hole spacings shall be complied with

- hole spacing in direction of force ≥ 3d
  ≥ 20 mm
- hole spacing at right angles to direction to force ≥ 30 mm
- hole spacing p ≥ 4d
  ≥ 40 mm
  ≥ 10d

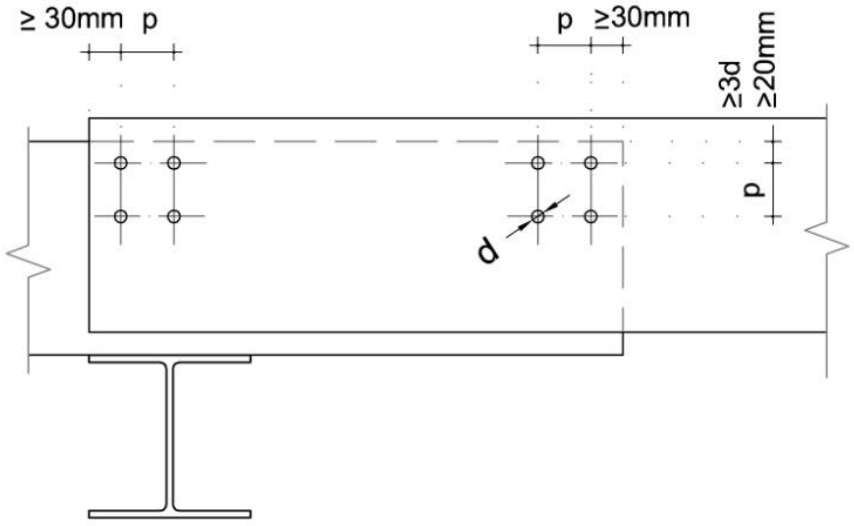

Fig. 20: the distances of the fasteners according to DIN 18807-3 for a statically effective overlapping

2.3 Conclusion

There are design procedures in DIN 18807 and further in EN 1090-4. The design rules are similar to each other. To confirm this procedure there should be a series of tests at the clamped joint to confirm this design procedure. In addition there should be a number of tests at the overlap joint to acquire data about the load bearing capacity.

3 Corrugated sheets

3.1 Component description

Corrugates steel sheets are the oldest cold formed steel sheets, they have a continuous curve instead of the flat sections like trapezoidal profiles.

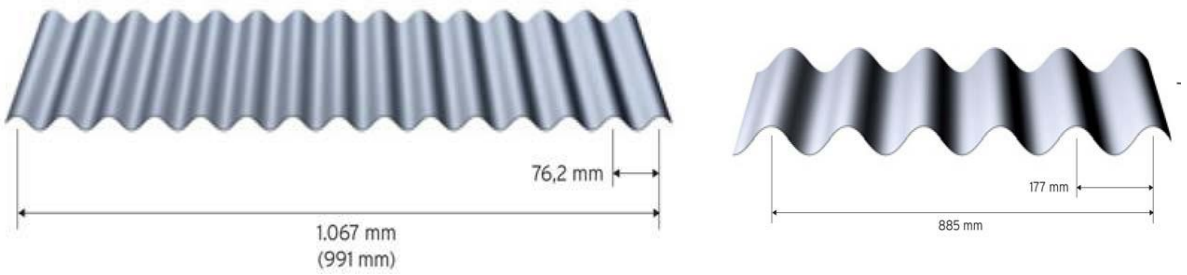

Fig. 21: Corrugated sheets

3.2 State of the art

The conventional bending theory can be used for corrugated steel sheets, because of the continuous curvature no local buckling is to be expected. In DIN 59231 [12] is a parameter range of the d/r-ratio where no buckling is expected.
In [13] there`s a calculation method which is developed from the comparison with FE calculations. This procedure corresponds to the usual procedure for buckling problems. Parameters are developed from the comparison with FE calculations with which the reduction factor χ between the limits for flat plates and circular cylinders can be calculated. With the help of this reduction factor χ you get finally the bearing stress of the cylinder segment. I. a. the influence of the boundary conditions of the longitudinal edges and various forms of predeformations are investigated.
It remains to check whether corrugated profiled sheets fit into the curvature of field of CTICM study. The different steps are shown in the following:

- Parameter of curvature:

$$Z = \frac{b^2}{R * t}$$

- critical buckling strength:

$$\sigma_{cr}{}^{z} = k_c^z * \sigma_E$$

with

$$\sigma_E = \frac{\pi^2 * E}{12 * (1-\nu^2)} * \left(\frac{t}{b}\right)^2 \quad \text{and} \quad k_c^z = \frac{k_c^{plate}}{2} * \left(1 + \sqrt{1 + \frac{48 * (1-\nu^2)}{\pi^4 * \left(k_c^{plate}\right)^2} * Z^2}\right)$$

- parameters$\bar{\lambda}$, β, $\overline{\lambda_0}$ and $\alpha_{z,s}$:

$$\bar{\lambda} = \sqrt{\frac{f_y}{\sigma_{cr}^{Z}}}$$

$$\beta = \frac{1 + 0{,}97^{Z}}{2}$$

$$\overline{\lambda_0} = 0{,}2 + 0{,}473 * 0{,}95^{Z}$$

$\alpha_{z:}$ table:

Z	0	10	20	30	≥40
α_z	0,28	0,38	0,33	0,21	0,13

- reduction coefficient χ

$$\chi = \frac{2 * \beta}{\beta + \bar{\lambda} + \sqrt{(\beta + \bar{\lambda})^2 - 4 * \beta * \left(\bar{\lambda} - \alpha_z * (\bar{\lambda} - \overline{\lambda_0})\right)}}$$

- ultimate stress σ_u

$$\sigma_u = \chi * f_y$$

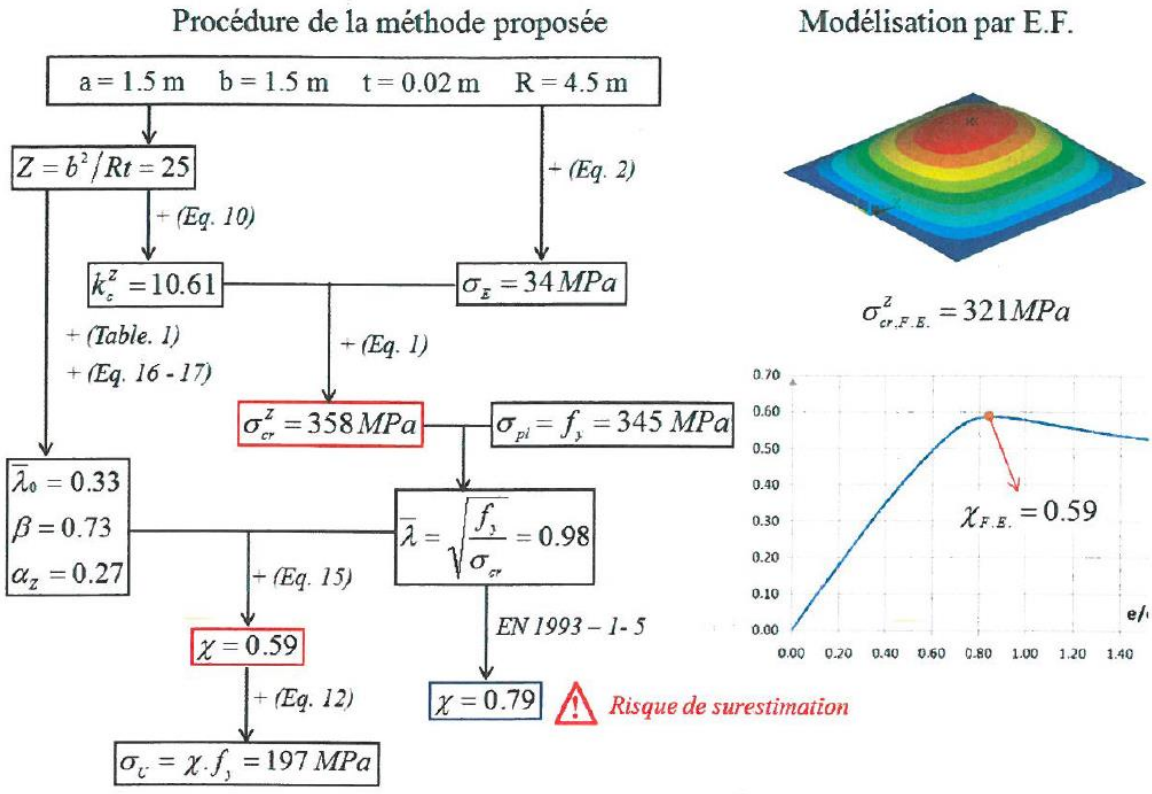

Fig. 22: An example of the proposed calculation method [13]

The effective second moment of area can be determined with the following approximate function

$$I = I_{eff} = \frac{2}{105} * h^2 * n * b_r * t * \left(\frac{1}{\cos\left(\arctan\left(\frac{4 * h}{b_r}\right)\right)} + 6 \right)$$

This equation is based on a parabolic curvature. The geometrical parameters n, h and b_r are explained in the following figure.

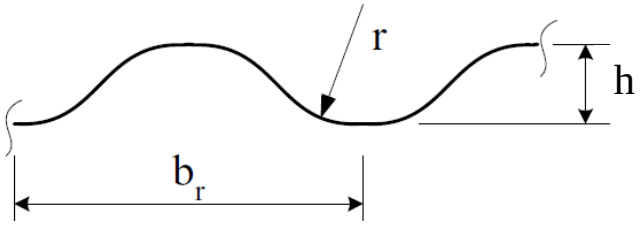

Fig. 23: Corrugated sheet

In DIN EN 1993-4-1 there`s another equation to determine the stiffness of corrugated sheets in steel silos. The stiffness for axial compression can be determined with the following equation

$$C_y = E * t * \left(1 + \frac{\pi^2 * d^2}{a * l^2}\right)$$

The second moment of area can be determined with the notation from shell structures with the following equation to

$$I_y = 0{,}13 * t * d^2$$

With the notation according to DIN EN 1993-1-3 you receive

$$I_x = 0{,}13 * t * {h_w}^2$$

Therefore moment resistance $M_{c,Rd}$ can be obtained with the following equation

$$M_{c,Rd} = \frac{130 * t * {h_w}^2}{\frac{h_w}{2}} * \frac{f_{yb}}{\gamma_{m0}} \quad (\text{Nmm/mm})$$

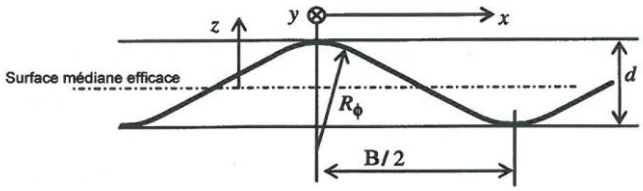

Fig. 24: corrugated sheet according to DIN EN 1993-4-1

Normally the corrugated sheets are designed by testing.
The tests are in accordance with DIN 18807 (see 1.3). Further informations are given in [14].

The pull-through resistance of fixings of steel sheeting can be determined according to DIN EN 1993-1-3 with

$$R_k = t * d_w * f_u * \alpha_{cycl} * \alpha_E$$

with

t	steel thickness
d_w	washer diameter
f_u	tensile strength
α_{cycl}	parameter for cyclic loads due the tensile loads (e.g. wind loading)
α_E	parameter for special cases of application

At the KIT tests with V-shaped specimen were recalculated and evaluated statistically (see fig. 16).

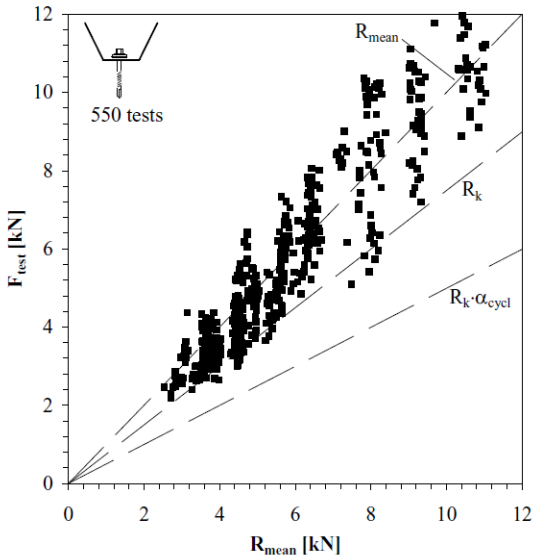

Fig. 25: Comparison of calculated load-bearing capacity with test results.

The characteristic value of load bearing capacity resulted in

$$R_k = 1{,}12 * t * d_w * f_u * \alpha_{cycl} * \alpha_E$$

The resistance can also be determined by tests. The test setups for trapezoidal and corrugated steel sheets are equal. Because the profile geometry for the profiled steel sheets treated in [15] has no or negligible influence. The standardized V-shaped specimen is shown in the following figure.

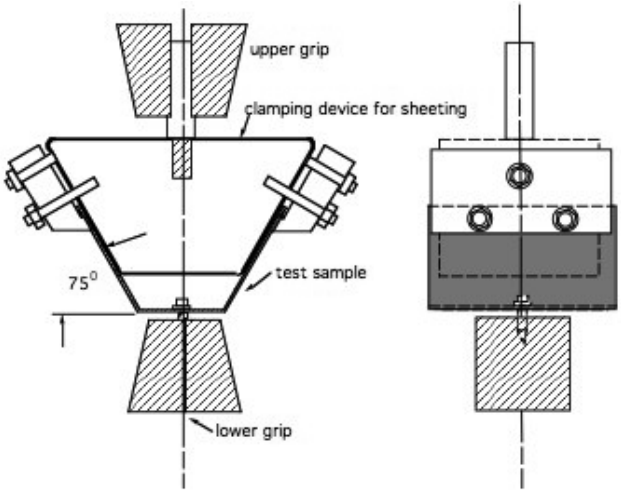

Fig. 26: Test setup according to [16]

3.3 Conclusion

There will be a number of test series to confirm the mentioned formulas and equations.

4 Curved profiles

4.1 Component description

There are three forms of curved profiles. The difference between the three forms is the method of curving. The shaping can be done by roll forming the profiles, by crushing the inner flange of the profiles or by bending the profiles on site.

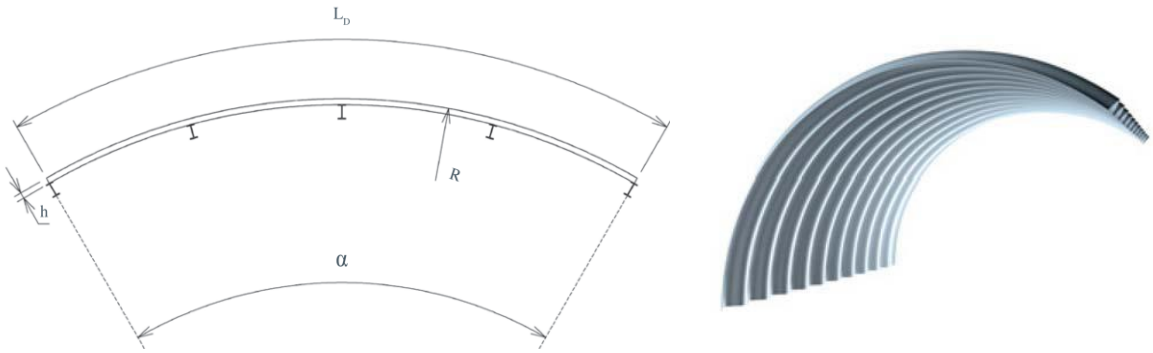

Fig. 27: curved profile by roll forming (variant A)

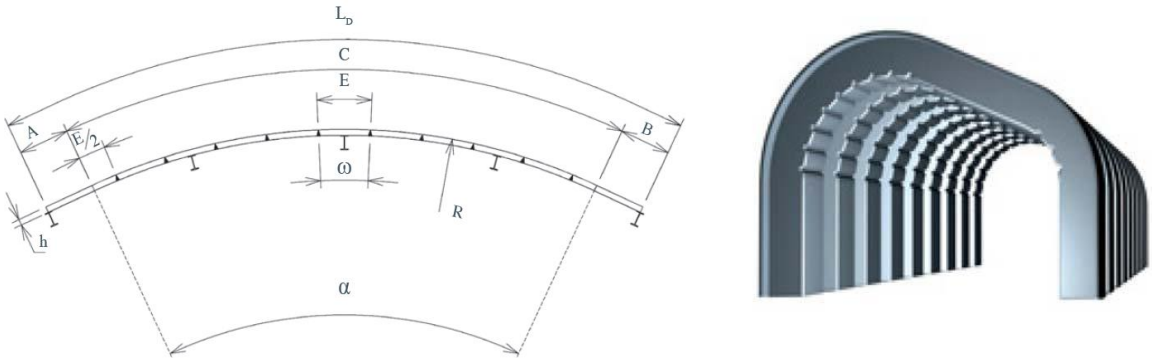

Fig. 28: curved profile by crushing the inner flange (variant B)

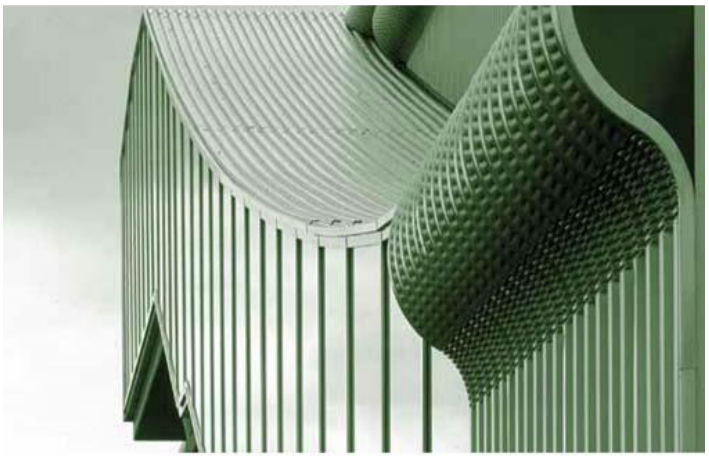

Fig. 29: curved profile by bending on site (variant C)

4.2 State of the art

Curved profiles

The bending load bearing capacity of variant B is not important because of the small spans.
Variant C can be designed according to the EN 1993-1-3 because of the large bending radius. Here, no change is expected in the bearing capacity compared to conventional profiles. There will be a focus on variant A in this project. In the following only variant A is considered.
The influence of residual stresses from the manufacturing was examined in the past at the research center of steel, timber and masonry in Germany.
A variety of tests according to DIN 18807-2 on curved trapezoidal profiles from different producers were performed. The bending radius was between 4 m and 19 m. The supports were not both fixed in the tests.
The difference in bending bearing capacity between a plane profile and a curved profile was between zero and ten percent.
In the literature you can find a reduction in the bearing capacity by 20% (narrow flange in compression) to 30% (wide flange in compression) [17].
If both supports are fixed, the bending theory is no longer applicable, the profile behaves like an arch.

Arch profiles

The arch actions produce high normal forces in the profile and thus high horizontal loads acting on the supports. These should be compensated by the substructure. Usually these systems are executed with tie rods. These compensate the horizontal arch forces from surcharges so that the substructure is merely loaded vertically, not taking into account wind suction load.
The company "Hoesch Building systems" has such a system developed in the past, it`s called "Legato Arch System".

Fig. 30: Hoesch arch roof [www.hoesch-bau.com]

In DIN 18807-3 there is an interaction formula for bending and normal force in trapezoidal profiled sheets.

In case of compression force the following is applied

$$\frac{N_D}{N_{dD}} * \left[1 + 0{,}5 * \alpha \left(1 - \frac{N_D}{N_{dD}}\right)\right] + \frac{M}{M_d} \leq 1$$

in case of tension force

$$\frac{N_Z}{N_{dZ}} + \frac{M}{M_d} \leq 1$$

is applied with

N_Z design value of tensile force
N_D design value of compressive force
M design value of bending moment
M_d design resistance of bending moment
N_{dZ} design resistance of tensile force
N_{dD} design resistance of compressive force

and

$$\alpha = \frac{L_{cr}}{i_{ef} * \pi} * \sqrt{\frac{f_{y,k}}{E}}$$

with

L_{cr} buckling length
i_{ef} radius of inertia of the effective cross section

4.3 Conclusion

There will be a number of test series to confirm the mentioned formulas and equations.
This will be the influence of the curvature by the curved profile and the verification of the interaction formula by the arch.

5 References

[1] Davies J. M. (2006b). Light gauge steel cassette wall construction – theory and practice, Journal of Constructional Steel Research, 62 (2006)
[2] Baehre R., Buca J. (1986). Die wirksame Breite des Zuggurtes von biegebeanspruchten Kassetten, Stahlbau 55 (9), 1986
[3] Baehre R. (1987). Zur Schubfeldwirkung und –bemessung von Kassettenkonstruktionen, Stahlbau 56 (7)
[4] Baehre R., Buca J., Egner R. (1990). Empfehlungen zur Bemessung von Kassettenprofilen, R. Schardt Festschrift, University of Darmstadt
[5] Davies J. M., Dewhust D.W. (1997). The shear behavior of thin-walled cassette sections infilled with rigid insulation, Proceedings of International Conference on Experimental Model Research and Testing of Thin-Walled Structures, Prague, Czech Republic, September 1997)
[6] Davis J. M., Fragos A. S. (2002). The local shear buckling of thin-walled cassettes infilled by rigid insulations – 1. Tests, proceedings of 3th European Conference on Steel Structures – Eurosteel 2002, Coimbra, Portugal 19-20 September (2002)
[7] Davies J. M., Fragos D.W. (2004). The local shear buckling of thin-walled cassettes infilled by rigid insulation, Journal of Constructional Steel Research, 60 (3-5)
[8] Davies J. M. (2002). Cassette wall construction, Current Research and Practice – Advance in Steel Structures – ICASS`02, Vol. 1(Chan S.L., Teng J.G. and Chung K.F., Eds), Elsevier Ltd., Oxford
[9] Voutay P.A., Davis J.M. (2002). Analysis of Cassette Sections in compression, Current Research and Practice – Advance in Steel Structures – ICASS`02, Vol. 1 (Chan S.L., Teng J.G. and Chung K.F., Eds.), Elsevier Science Ltd., Oxford
[10] Jönsson J., Ramonas G. (2012). Flange curling in cold formed profiles – Nordic Steel Construction Conference 2012, Hotel Bristol, Oslo Norway 5-7 September (2012)

[11] Bernard E.S., Bridge R.Q. (1995). Flange curling in profiled steel decks – Thin-Walled Structures
[12] DIN 59321 2003:11. Wellbleche und Pfannenbleche
[13] Le Tran K., Davaine L., et al.: Etude de la Resistance et de la Stabilite des Panneaux cylindriques non-raidis soumis a une Compression uniforme: application aux ouvrages d`arts, Revenue Construction Metallique, 01-2012
[14] Touchard, R.: Wellbleche, moderne Bauelemente mit genormter Tragfähigkeit. Deutscher Verzinkerei Verband e. V., Düsseldorf, Dezember 1988
[15] Misiek. T., et al.: Pull-through resistance of tensile-loaded srew-fastenings of thin-walled sheeting and sandwich panels, Stability and Ductility of Steel Structures, Rio de Janeiro, Brazil, 8-10 September
[16] ECCS TC 7, The Testing of Connections with Mechanical Fasteners in Steel Sheeting and Sections, ECCS publication no. 124, Brussels, 2009.
[17] James L. Jorgenson J.L., Chowdhury A.H.. Buckling Strenght of cold formed steel curved panels